# MFG-E8 promotes M2 polarization of macrophages and is associated with poor prognosis in patients with gastric cancer

Yang Li [a], Jianda Qiu [a], Ziyu Meng [a], Shiyuan Yin [a], Mingxuan Ruan [a], Wenbiao Zhang [a], Zhiwei Wu [a], Tao Ding [a], Fei Huang [b,**], Wenbin Wang [a,*]

[a] *Department of Surgery, The First Affiliated Hospital of Anhui Medical University, Anhui Public Health Clinical Center, Hefei, People's Republic of China*
[b] *Department of Orthopaedics, The Second Affiliated Hospital of Anhui Medical University, Hefei, People's Republic of China*

## ARTICLE INFO

## ABSTRACT

*Background:* Milk Fat Globule-Epidermal Growth Factor 8 (MFG-E8) has been reported to play an oncogenic role in a variety of tumors. However, its involvement in gastric cancer (GC) development has not been described.
*Methods:* The cancer genome atlas (TCGA) and the gene expression omnibus database (GEO) databases were used to analyze the expression of MFG-E8 in GC. These findings were further validated using immunohistochemistry (IHC) and western blotting assay (WB). Kaplan-Meier method, univariate logistic regression, and Christopher Cox regression were used to study the relationship between MFG-E8 and clinical pathology. In addition, the potential signaling pathways involved in MFG-E8 and its potential correlation with levels of immune cell infiltration were investigated. Finally, the biological function of MFG-E8 in GC cells was revealed.
*Results:* MFG-E8 was highly expressed in GC patients and cells, and the high level of MFG-E8 was associated with poor overall survival (OS). KEGG analysis indicated that MFG-E8 may play an important role in the cAMP signaling pathway. The expression of MFG-E8 was positively correlated with the infiltration of M2 macrophages. The patients with high MFG-E8 were easy to develop chemotherapy resistance. Furthermore, the knockdown of MFG-E8 significantly inhibited the proliferation and invasion of GC cells.
*Conclusion:* MFG-E8 in GC may serve as a prognostic marker and a potential immunotherapy target for GC.

## 1. Introduction

Gastric cancer (GC) has more than one million new cases each year, 700,000 of which occur in developing countries, and is the fifth most common cause of the disease nationwide [1,2]. With the improved understanding of GC molecules in recent years, we have come to believe that cancer may have unique pathogenic mechanisms and abundant oncogenic pathways. Based on these reasons, finding

---

* Corresponding author. Department of Surgery, The First Affiliated Hospital of Anhui Medical University, Anhui Public Health Clinical Center, Hefei, People's Republic of China.
** Corresponding author. Department of Orthopaedics, The Second Affiliated Hospital of Anhui Medical University, Hefei, Anhui, 230000, People's Republic of China.
*E-mail addresses:* huangfei3739@163.com (F. Huang), wwb202310@163.com (W. Wang).

and identifying molecular markers associated with GC occurrence can clarify the clinical features of GC and thus predict the consequences such as recurrence and metastasis of GC patients, which is an important goal of GC research [3,4].

Milk fat globule-EGF factor 8 (MFG-E8) is a peripheral membrane protein [5]. It was first identified in the lactating mammary glands of mice and is also present in many other cell types. The N-terminal end of MFG-E8 binds to integral proteins on the cell membrane surface via the arginine-glycine-aspartate (RGD) integrin sequence in the epidermal growth factor-like (EGF) structural domain, which in turn can regulate intercellular adhesion, invasion, and apoptosis [6]. At its C-terminus, it is able to specifically bind to the phospholipid bilayer on the cell membrane surface due to the tyrosine kinase receptor F5/8C structural domain [7,8]. It has been found that exposure of phosphatidylserine (PS) to the outside surface of cell membranes is a major feature of apoptotic and dead cells. Many investigators have demonstrated that MFG-E8 is an important factor in the development of various inflammatory diseases. For example, it can prevent osteoarthritis by targeting chondrocytes through the NF-KB pathway to delay senescence and promote macrophage M2 polarization [9–12]. Several studies recently have also found that it plays an important part in multiple kinds of malignant tumors, like breast cancer [13], as well as in colorectal cancer [14], ovarian cancer [15], melanoma [16], and others. Nevertheless, the expression and function of MFG-E8 in GC remain unknown.

The tumor-associated macrophages (TAMs) in the tumor immune microenvironment (TIME) play an important role in the development of tumors [17]. TAMs fall into two types: M1, which promotes inflammation, and M2, promotes cancers [18]. Therefore, the effective inhibition of M2 macrophages in cancer therapy has attracted more and more attention [19]. Recent studies have shown that MFG-E8 induces macrophage M2 polarization through the SOCS3/STAT3 signaling pathway, accelerating the repair of spinal cord injury (SCI) [20]. In addition, MFG-E8 promotes angiogenesis in melanoma by enhancing the M2 polarization of macrophages [21].

In this study, we comprehensively explored the association between MFG-E8 expression and the prognostic value of GC patients using the cancer genome atlas (TCGA) and the gene expression omnibus database (GEO). In addition, the signaling pathways involved in MFG-E8 and their correlation with immune cell infiltration and predictions for drug sensitivity analysis will be analyzed. Finally, MFG-E8 was knocked down in AGS and MKN-45 cells and performed EDU, wound healing, and Transwell invasion assays to further validate the pro-cancer role of MFG-E8 in GC.

## 2. Methods

### 2.1. Data collection

Pan-cancerous mRNA Transcripts Per Million (TPM) data were downloaded from the TCGA database, where the TCGA-STAD dataset contains 375 GC tissues and 32 normal tissues. In addition, the GEO database was used to validate the expression of MFG-E8, the data included the GSE54129 data set (21 normal and 111 tumor tissues) and the GSE79973 data set (10 Paracancerous and 10 tumor tissues). The data were visualized by R software (version 4.2.1).

### 2.2. Clinical samples

A total of 40 GC tumors and adjacent tissues were obtained from the First Affiliated Hospital of Anhui Medical University. Fresh specimens from patients were saved in liquid nitrogen immediately after surgery. The pathological characteristics of the specimens had been analyzed by two independent pathologists according to the guidelines established by the World Health Organization ( WHO ) . The study protocol obtained approval from the ethics committee of the First Affiliated Hospital of Anhui Medical University. All the patient samples and clinical data involved in this study were in accordance with the Declaration of Helsinki.

### 2.3. Correlation analysis of prognosis

Based on the clinicopathological features and survival data of GC in the TCGA database, the GC patients were divided into high and low groups according to the expression of MFG-E8. The relationship between the high group and the low group was analyzed by the ggplot2, stats, and car package of R. Kaplan Meier analysis was used to visualize the prognosis of GC patients. The ability to predict the prognosis of GC patients was assessed using receiver operating characteristic curves (ROC) generated by timeROC and ggplot2 packages. In addition, we performed univariate and multivariate Christopher Cox regression analyses, and hazard ratios for MFG-E8 expression and clinicopathological features were obtained. On this basis, we constructed nomograms to predict the OS of GC patients, using survival, rms package in R for analysis and visualization.

### 2.4. GO and KEGG pathway enrichment analyses of differential expression genes

Differential expression genes (DEGs) analysis between these two groups was performed using the DESeq2 package in R. Select | log2-fold-change (FC)| > 1 with an adjusted p-value <0.05. Volcano plots and co-expression heatmaps were plotted using the ggplot2 package (the top 30 positively correlated proteins were selected). In addition, Gene Ontology (GO) and Kyoto Encyclopedia of Genes and Genomes (KEGG) enrichment analyses were performed using the ClusterProfiler R package.

### 2.5. Immune infiltration analysis

First, based on the expression data of samples in the TCGA-GC dataset, the immune cell content in each sample was evaluated by the

CIBERSORT algorithm. Secondly, the expression data of MFG-E8 was extracted by calculating the score of each sample in stromal cells and immune cells by estimate package, the differences of MFG-E8 expression in stromal cells, immune cells, and total score were obtained. The correlation between the MFG-E8 gene and 24 kinds of immune cells was analyzed based on the GSVA package in R. The relationship between MFG-E8 and macrophage subtypes was evaluated by the CIBERSORT algorithm. Finally, the relationship between MFG-E8 expression and macrophage prognosis was evaluated by tumor immune estimation resource (TIMER). The correlation between MFG-E8 and M2 macrophage marker was analyzed, and the results were visualized using the ggplot2 package in R.

### 2.6. Cell culture

GC cell lines (AGS, MKN-45) and human gastric mucosal cells (GES-1) were purchased from the Shanghai Cell Bank, Chinese Academy of Sciences. The cell culture medium consisted of RPMI-1640 medium (Corning, USA), 10 % fetal bovine serum (Gibco; Thermo Fisher Scientific, USA), and 100 U/ml penicillin, 100 U/ml streptomycin (90 %:10 %:1 %). Then, we incubated in an incubator at 37 °C with 5 % $CO_2$. The medium was changed every 3 days.

### 2.7. Immunofluorescence staining

AGS cells were spread on coverslips of 24-well plates and cultured in the complete medium under cell culture conditions. Cells were fixed with 4 % paraformaldehyde for 10 min at room temperature and then punched with 0.1 % Triton-100 for 8 min at room temperature. Cells were blocked in 2 % BSA for 45 min, washed in 1 × PBS, and stained with phalloidin (diluted with 2 % BSA) for 30 min at room temperature. After a brief wash in 1 × PBS, cells were incubated overnight at 4 °C with a human monoclonal anti-MFG-E8 antibody (Santa Cruz, USA), diluted 1:200 in 2 % BSA. After cell washing, cells were incubated with goat anti-mouse IgG diluted 1:400 in 2 % BSA with Alexa fluor488 (Invitrogen, USA) for 1 h at room temperature. After washing with 1 × PBS, cells were stained with DAPI for 2 min and visualized by confocal microscopy.

### 2.8. Immunohistochemistry

We first cut the paraffin-embedded GC specimens into roughly 4–5 μm sections. The slices were baked in a 65 °C oven for 2 h before the experiment. The sections were then dewaxed twice in xylene for 15 min each. They were hydrated in an alcohol gradient (100 %, 95 %, 80 %) for 5 min each time. Finally, they were rinsed with deionized water. Following the antibody instructions, antigen repair was performed using citrate buffer and blocked using endogenous peroxidase. The sections were then incubated with an MFG-E8 antibody (1:4000 dilution, Proteintech, China) overnight at 4 °C, followed by a secondary antibody (Proteintech, China) for 30 min at normal temperature. Sections were rinsed twice using Phosphate Buffered Saline (PBS), followed by DAB staining, and finally restained with hematoxylin. The results were evaluated based on the intensity of staining (I), classified as none (0), weak (1), moderate (2), or strong (3), and the percentage of positive results (P), classified as 1: 1–25 %, 2: 26–50 %, 3: 51–75 %, or 4: 76–100 %. The product value of I and P was between 0 and 6 for the low-expression group and between 7 and 12 for the high-expression group, and the results were evaluated accordingly.

### 2.9. siRNA transfection

Knockdown of MFG-E8 expression in AGS and MKN-45 cells was performed. The specific siRNA was synthesized in Tsingke Bio-technologyCo.,Ltd. (Nanjing, China). The sequences were as follows: si-MFGE8-1(sense):5′-GGAACATTGCCAACTCACA-3′, si-MFGE8-2 (sense):5′-GGACACGAATTCGATTTCA-3′ and si-Control (sense):5′-TTCTCCGAACGTGTCACGT-3′. The siRNA was transfected into GC cells using Lipo2000 (Invitrogen, USA) with non-targeting siRNA NC as control. The transfected cells were cultured at 37 °C for 4–6 h, then the fresh medium was changed. After 48 h of continuous culture, the following tests can be performed with the cells.

### 2.10. 5-Ethynyl-20-deoxyuridine (EDU) proliferation assay

GC cells transfected with siRNA were seeded into 96-well plates at $5 \times 10^4$/well. Next, 100 μl of EDU (KeyGEN BioTECH, Nanjing, China) working solution with a final concentration of 10 μm was added to each well to culture cells. After a period of culture, the cells were fixed in 4 % formaldehyde, infiltrated with 0.5 % TritonX-100, and then incubated with 100 μL of EDU mixture. The cells were then stained with 100 μl Hoechst 33342 and observed under an inverted Fluorescence microscope ( Zeiss, Germany). The number of EDU-positive cells (erythrocytes) was calculated by Image J software, and the EDU incorporation rate is expressed as the proportion of EDU-positive cells to total cells.

### 2.11. Wound healing assay

First, we used the marker pen to draw the horizontal line evenly. GC cells transfected with siRNA were plated in 12-well plates and grown to fusion. Then, after 24 h of cell starvation, we made a horizontal wound using a 10 μL pipette tip. We then captured the wounds and measured their width under a light microscope at 0 and 24 h after the cuts.

### 2.12. Transwell invasion assay

For this assay, a 24-hole Transwell chamber (Corning, USA) was used. Matrigel (Sigma-Aldrich, USA) diluted with serum-free RPMI 1640 was added vertically to the upper chamber while cells were also seeded into the upper chamber, and 500 μL of RPMI 1640 medium was added to the basolateral chamber, it was then cultured at 37 °C for 24 h. We then fixed the cells with 4 % para-formaldehyde and stained them with 0.1 % crystal violet dye. Next, place the chamber in 1 × PBS and carefully swab the cells and gel from the upper chamber with a cotton swab. Finally, 5 fields were selected for cell counting and the results were analyzed under an inverted microscope (Zeiss, Germany).

### 2.13. Western blotting method

Total cellular proteins were extracted from cells (GES-1, MKN45, AGS). A 10 % sodium dodecyl sulfate-polyacrylamide gel (SDS-PAGE) was first prepared, and then approximately 25 μg of protein samples were added to each well. Next, electrophoresis, membrane transfer, 5 % milk blocking, and finally incubation with MFG-E8 antibody (1:300 dilution, Santa Cruz Biotechnology, USA) overnight in a 4 °C shaker were performed. The next day the secondary antibody (1:4000 dilution, Proteintech, China) was washed for 10 min using TBST and next incubated at room temperature. Finally, the signal was detected using BeyoECL Moon (beyotime, China).

### 2.14. Predictions for drug sensitivity analysis

The OncoPredict R package, designed by Maeser and colleagues, includes a repertoire of 198 chemotherapy drugs, with the primary aim of predicting drug responses in cancer patients. Prior to conducting the analysis, two essential files must be prepared. The first file is the gene expression profile obtained from the TCGA database. The second file is the Genomics of Drug Sensitivity in Cancer (GDSC) matrix. This matrix encompasses data for half-maximal inhibitory concentrations (IC50) of cancer cells.

To further assess how drug sensitivity changes with varying levels of MFG-E8 expression, two essential files are required: one is the gene expression profile downloaded from the TCGA database, and the other is the drug sensitivity data obtained through OncoPredict R analysis. All analyses were conducted using the R (version 4.2.1).
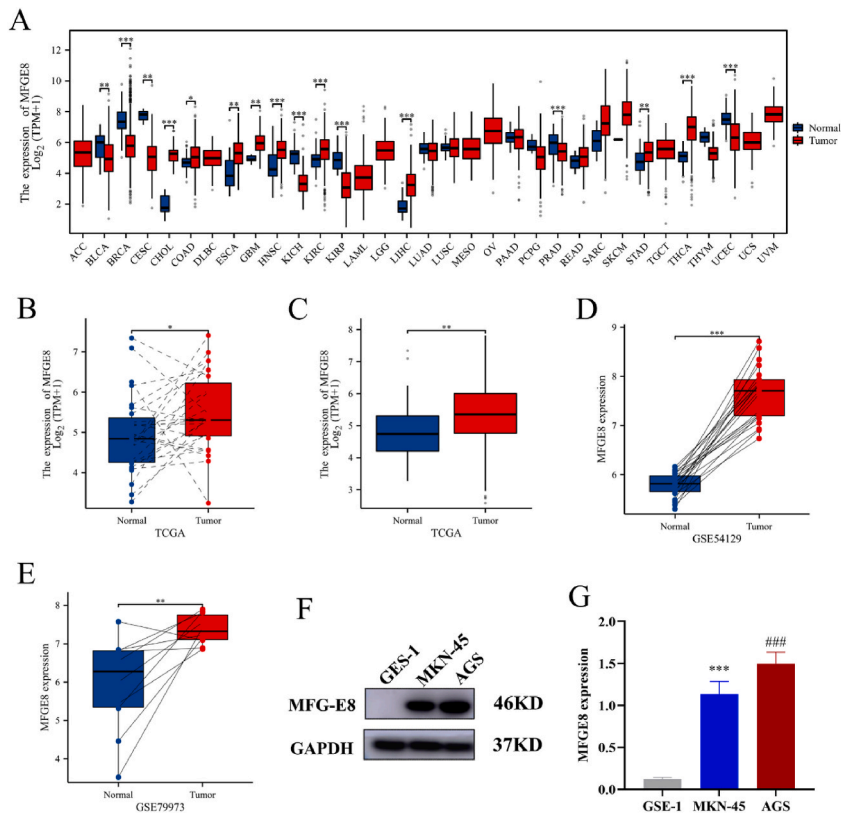


**Fig. 1.** Expression of MFG-E8 in GC tissues and cells. (A) Expression levels of MFG-E8 in pan-carcinomas based on the TCGA database. (B) Comparison between GC and paired normal tissues in the TCGA database. (C) Comparison between GC and unpaired normal tissues in the TCGA database. (D) Comparison between GC and unpaired normal tissues in GSE54129. (E) Comparison between GC and paired normal tissues in GSE79973. (F, G) WB assay was used to detect the protein level of MFG-E8 in GC cells. *p < 0.05, **p < 0.01, ***p < 0.001, ###p < 0.001.

### 2.15. Statistical analysis

Statistics from TCGA and GEO databases were analyzed using R software (version 4.2.1). Wilcoxon rank-sum test was used to analyze the correlation between MFG-E8 expression and pathological features. Univariate Cox and multivariate Cox regression analyses were combined to evaluate the independent prognostic value of MFG-E8 expression. $P < 0.05$ was considered statistically significant.

## 3. Results

### 3.1. Expression of MFG-E8 in different types of human tumors

Based on the TCGA database, we first analyzed MFG-E8 in pan-cancer. As shown in Fig. 1A, MFG-E8 expression in cholangiocarcinoma (CHOL), colon adenocarcinoma (COAD), esophageal carcinoma (ESCA), glioblastoma multiforme (GBM), head and neck squamous cell carcinoma (HNSC), renal clear cell carcinoma (KIRC), hepatocellular carcinoma (LIHC), thyroid cancer carcinoma (THCA), and gastric carcinoma (STAD) show high expression. MFG-E8 was highly expressed in 32 pairs of GC tissues (Fig. 1B). Furthermore, the expression of MFG-E8 in GC samples was significantly higher than that in normal tissues (Fig. 1C). In addition, the GSE79973 and GSE54129 data sets further confirmed this finding (Fig. 1D and E). We subsequently extracted proteins from GC cells and found by WB experiments that MFG-E8 was highly expressed in GC cells compared to gastric mucosal cells (Fig. 1F and G).

MFG-E8 was located by immunofluorescence assay. As shown in Fig. 2A, MFG-E8 is expressed in the cytoplasm and membrane [22]. Furthermore, we collected clinical samples and further verified by IHC experiments that MFG-E8 was expressed in the cytoplasm and cell membrane and upregulated in GC tissues (Fig. 2B and C).

### 3.2. The relationship between the expression of MFG-E8 and the clinicopathological features and prognosis of GC

As shown in Fig. 3A, high expression of MFG-E8 was significantly associated with the T stage (T1 vs. T2, T1 vs. T3, T1 vs. T4, $p < 0.001$). It was independent of age, N grade, and M grade. In addition, KM survival analysis showed that MFG-E8 expression was negatively correlated with age, T grade, and N grade (Fig. 3B).

### 3.3. Prognosis of MFG-E8 in GC and establishment of the Nomogram

Kaplan-Meier analysis was used to analyze the correlation between MFG-E8 expression and OS, and DSS in GC patients in TCGA. As
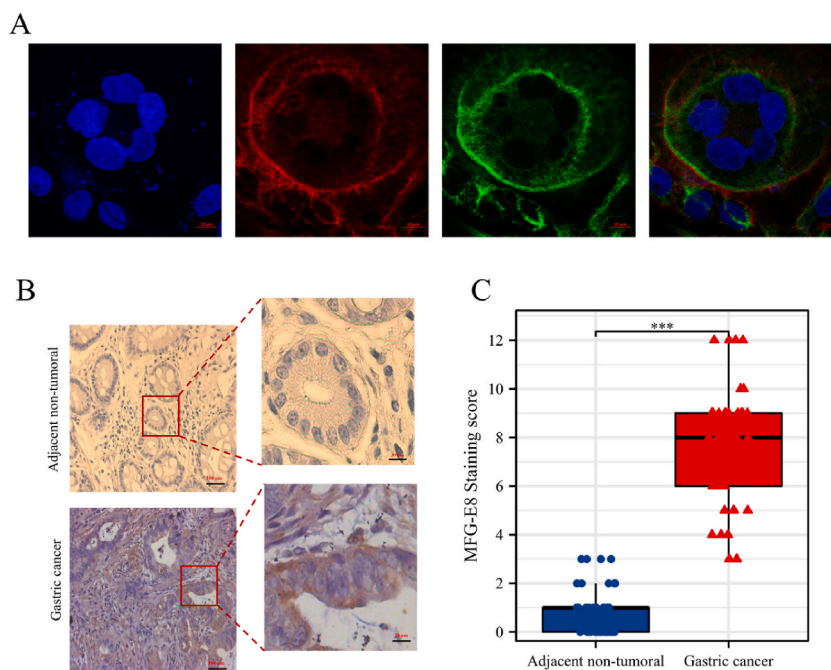


**Fig. 2.** Localization of MFG-E8 in cells and expression in GC tissues. (A) The localization of MFG-E8 in AGS cells was determined by immunofluorescence. (B, C) Expression of MFG-E8 in 40 tumors and adjacent tissues as determined by IHC (The nucleus was colored blue, MFG-E8 was labeled with green fluorescence, the cell morphology was colored red, and the merged result is shown in yellow; Magnification, × 200). (For interpretation of the references to color in this figure legend, the reader is referred to the Web version of this article.)
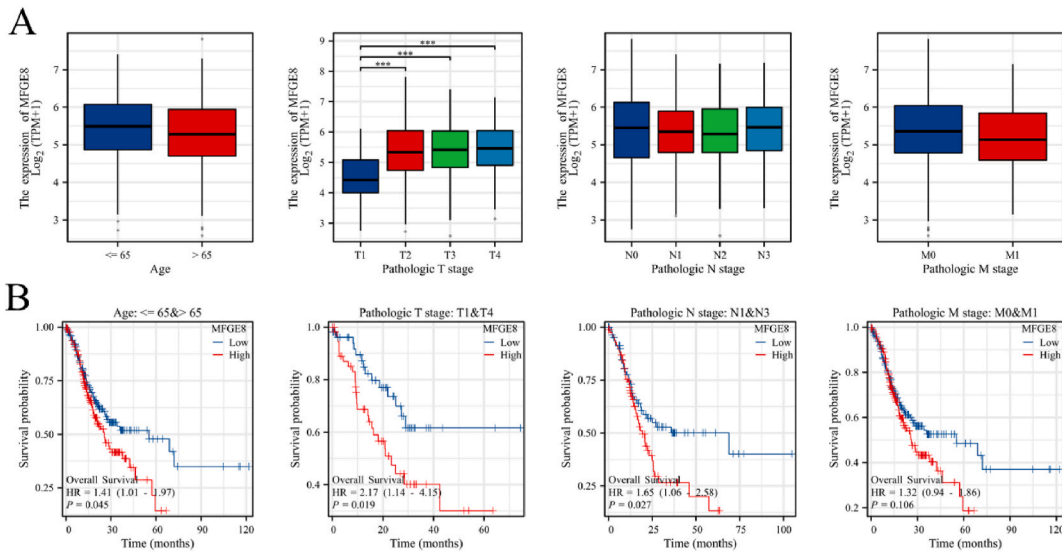
**Fig. 3.** Expression and prognosis of MFG-E8 in different subgroups of GC patients. (A) The relationship between high and low MFG-E8 expression and age, T classification, N classification, and M classification. (B) OS survival curves for high and low MFG-E8 with age >65 years, T1 and T4, N1 and N3, M0 and M1.

shown in Fig. 4A and B, MFG-E8 expression was inversely associated with OS and DSS (HR = 1.42, p = 0.042; HR = 1.56, p = 0.043). In addition, in the GC cohort of TCGA, we applied receiver operating characteristic (ROC) curves to predict AUC areas of 0.540, 0.614, and 0.815 for 1-, 3-, and 6-year OS, respectively (Fig. 4C). This suggests that MFG-E8 may be a potential biomarker for GC patients.
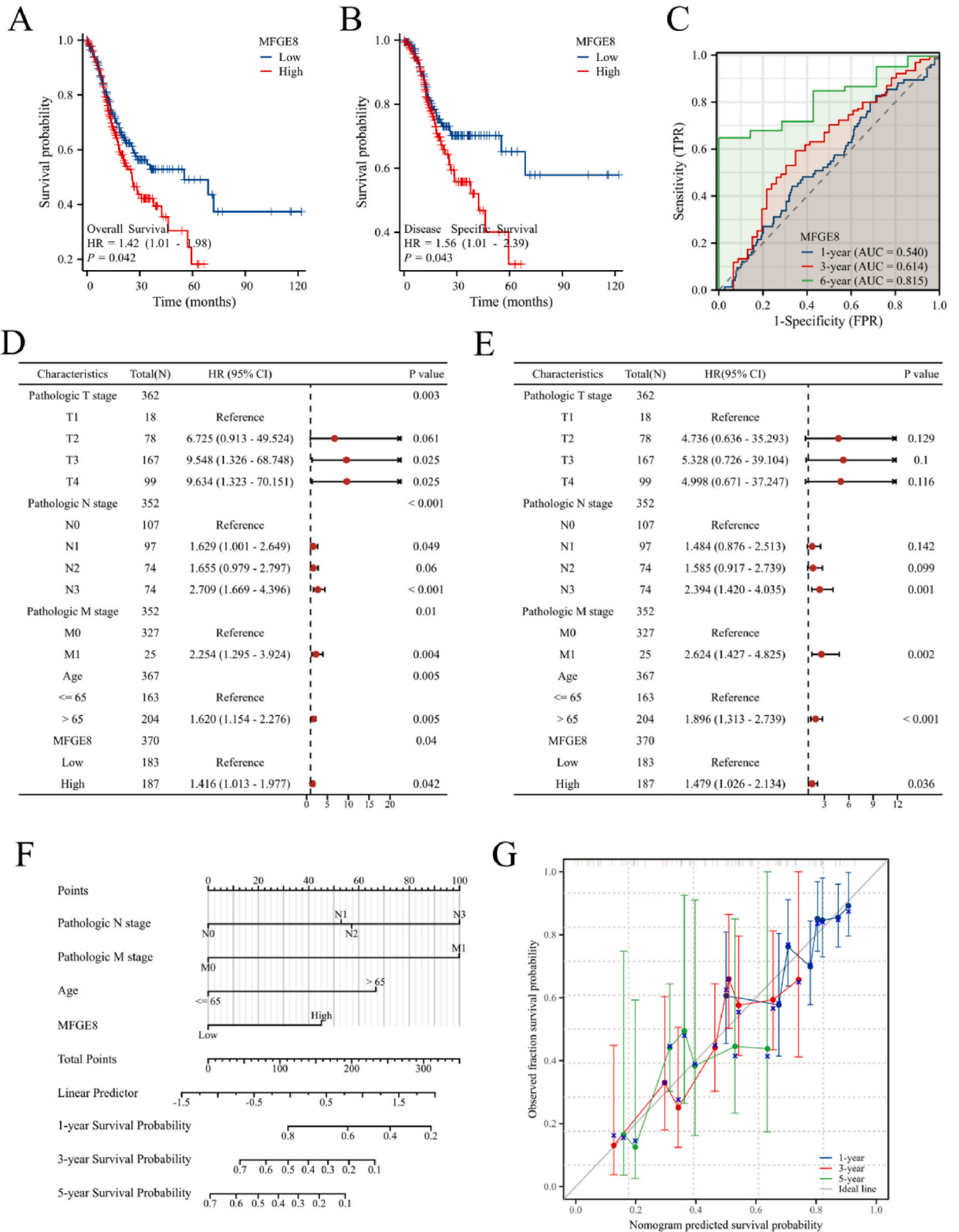
To plot Nomograms, we performed univariate and multivariate Cox regression analyses to determine prognostic indicators. As shown in Fig. 4D and E, N stage, M stage, age, and MFG-E8 expression were independent factors for OS in GC patients. According to the regression coefficient of the independent factor, the scoring standard is set, and the total score of each individual is calculated. On the Nomogram, higher total points were associated with a worse prognosis (Fig. 4F). In addition, calibration curves are used to assess the accuracy of nomograms. As shown in Fig. 4G, the predictions of the modeled nomograms were consistent with observations in GC patients.

### 3.4. Identification and functional enrichment analysis of MFG-E8-related DEGs in GC

As shown in Fig. 5A, a total of 2114 DEGs associated with MFG-E8 were identified, including 1160 up-regulated genes and 954 down-regulated genes. We selected the first 30 DEGs and rendered them as heat maps (Fig. 5B). To further investigate the function of DEGs in GC associated with MFG-E8 expression, we performed a functional enrichment analysis. As shown in Fig. 5C, the GO enrichment analysis focused on the following three areas: biological processes (BP) including Muscle system process, muscle contraction, and regulation of muscle system process; cellular components (CC) including contractile fiber, myofibril, Z disc; and biological processes (BP) including Muscle system process, muscle contraction, and regulation of muscle system process Molecular functions (MF) include hormone activity, structural constituent of muscle and acetylcholine receptor activity. KEGG enrichment analysis showed that MFG-E8 may be related to the Neuroactive ligand-receptor interaction, cAMP signaling pathway, Cholinergic synapse, and other pathways.

### 3.5. Analysis of immune infiltration related to MFG-E8 in GC

We first analyzed the proportion of immune cell subsets in each GC patient using the CIBERSORT algorithm (Fig. 6A). Then the expression of MFG-E8 in TCGA-GC was extracted and the relationship between MFG-E8 and the immune microenvironment (TMB) was analyzed. Results as shown in Fig. 6B, the MFG-E8 high expression group was upregulated in ImmuneScore, ESTIMATEScore, and StromalScore compared with the MFG-E8 low expression group. We subsequently had to utilize the ssGESA algorithm to compare the proportions of 24 immune cell subtypes between the low-MFG-E8 group and the high-MFG-E8 group, and our results again showed that MFG-E8 was significantly associated with immune cells (Fig. 6C). Furthermore, macrophage enrichment scores were significantly higher in the MFG-E8 high-expression group than in the MFG-E8 low-expression group (Fig. 6D and E). We further analyzed the relationship between MFG-E8 and macrophage subtypes using the CIBERSORT algorithm. As shown in Fig. 6F and G, MFG-E8 was positively correlated with M2 subtype macrophages. Finally, we used the TIMER database analysis to conclude that macrophage expression in GC was inversely correlated with OS (Fig. 6H).
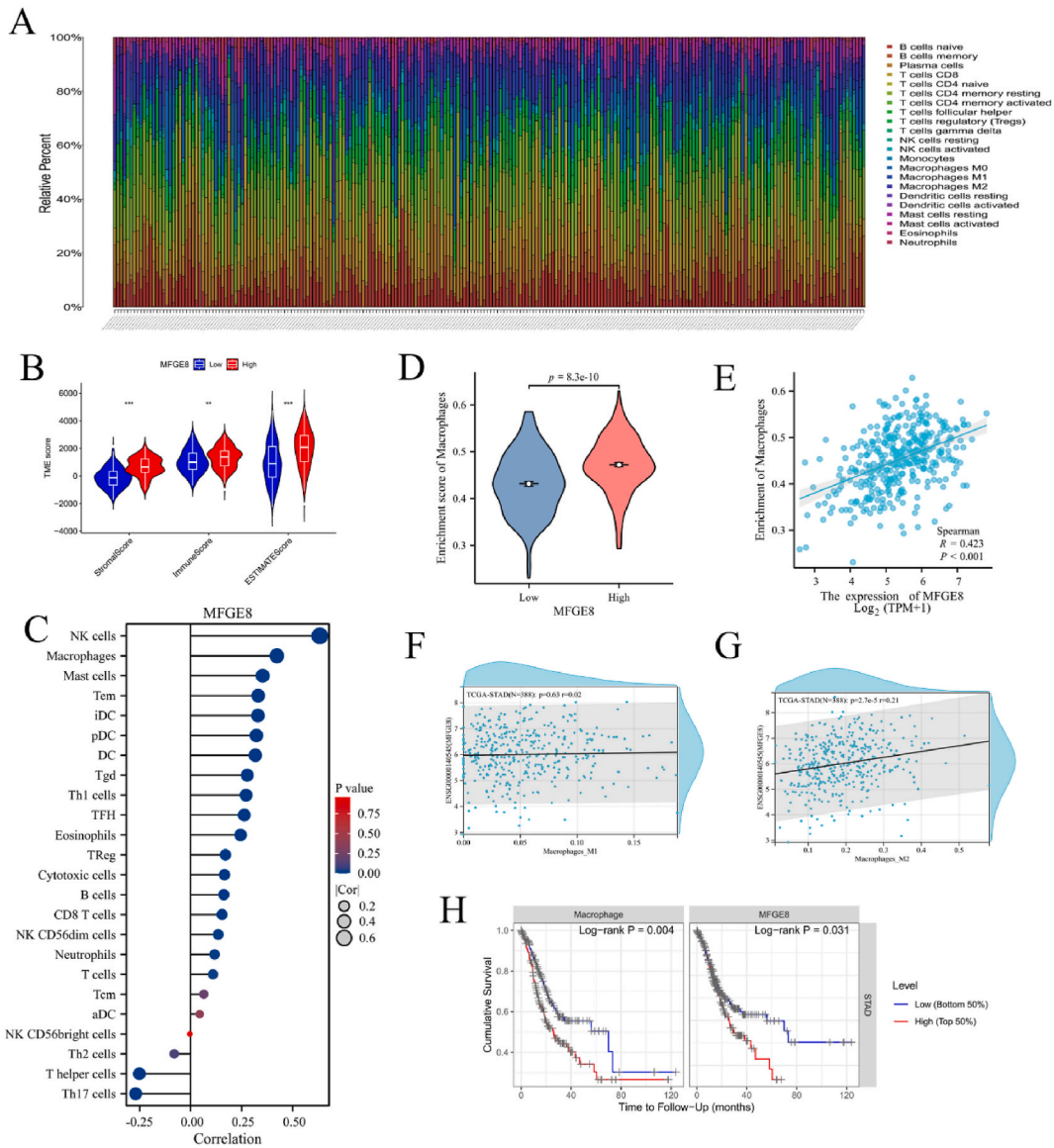
(caption on next page)

**Fig. 5.** Identification and functional enrichment analysis of differentially expressed genes (DEGs) related to MFG-E8 in GC. (A) Volcano map of DEGs. (B) Co-expression heatmap of DEGS. (C) GO and KEGG enrichment analysis of MFG-E8-related DEGs in GC. BP, biological Process; CC, cellular compositions; MF, molecular functions. ***p < 0.001.

### 3.6. Correlation between immune infiltration and MFG-E8 expression in GC

MFG-E8 is closely associated with immune cell infiltration. To verify this hypothesis, we conducted an analysis of the correlation between MFG-E8 and molecular markers for TAM (IL-10, CCL2, and CXCL8), M1 macrophages (RFX5, NOS2, and IFNG), and M2 macrophages (MRC1, CD163, and VSIG4). The results of the analysis revealed a positive correlation between MFG-E8 and IL-10 in TAM (rho = 0.339), with IL-10 being a factor secreted by M2 macrophages. In contrast, MFG-E8 showed no significant correlation with the infiltration levels of M1 macrophages (RFX5, rho = 0.164; NOS2, rho = 0.029; IFNG, rho = 0.022). However, MFG-E8 exhibited a positive correlation with the infiltration levels of M2 macrophages (MRC1, rho = 0.333; CD163, rho = 0.358; VSIG4, rho = 0.427) (see Fig. 7A–C). In summary, our findings indicate a close association between MFG-E8 and the polarization of M2 macrophages.

**Fig. 6.** The relationship between MFG-E8 and immune infiltration of GC. (A) The relative proportion of high and low MFG-E8 immune infiltrates. (B) The StromalScore, ImmuneScore, and ESTIMATEScore of TME differed between high and low MFG-E8 expression groups. (C) Correlation between MFG-E8 and the relative abundance of 24 immune cells in GC. (D) Comparison of immune infiltration levels of macrophages between high and low MFG-E8 expression groups. (E) Correlation between relative enrichment score of macrophages and MFG-E8 expression. (F, G) Relationship between MFG-E8 expression and macrophage subtypes. (H) OS survival curves of macrophages between high and low MFG-E8 expression groups. **p < 0.01, ***p < 0.001.

### 3.7. Correlation analysis between MFG-E8 and chemotherapeutic drugs in GC

We used the oncoPredict package to evaluate the relationship between MFG-E8 expression and the chemotherapeutic drugs commonly used in GC. Our analysis results showed that patients with high expression of MFG-E8 had low sensitivity to Dihydrorotenone, whereas they were sensitive to AZD1332 and Dasatinib (Fig. 8A). To better describe the relationship between MFG-E8 expression and drug IC50, we further mapped the scatter plot. Our results showed that the sensitivity to AZD1332 and Dasatinib increased with the increase of MFG-E8 expression (Fig. 8B).

### 3.8. MFG-E8 plays an important role in promoting GC

To verify whether MFG-E8 could play an important role as a pro-oncogene in GC, we knocked it down in GC cell lines using siRNA targeting human MFG-E8. To further explore the carcinogenic role of MFG-E8 in GC. First, we examined the mRNA expression levels of
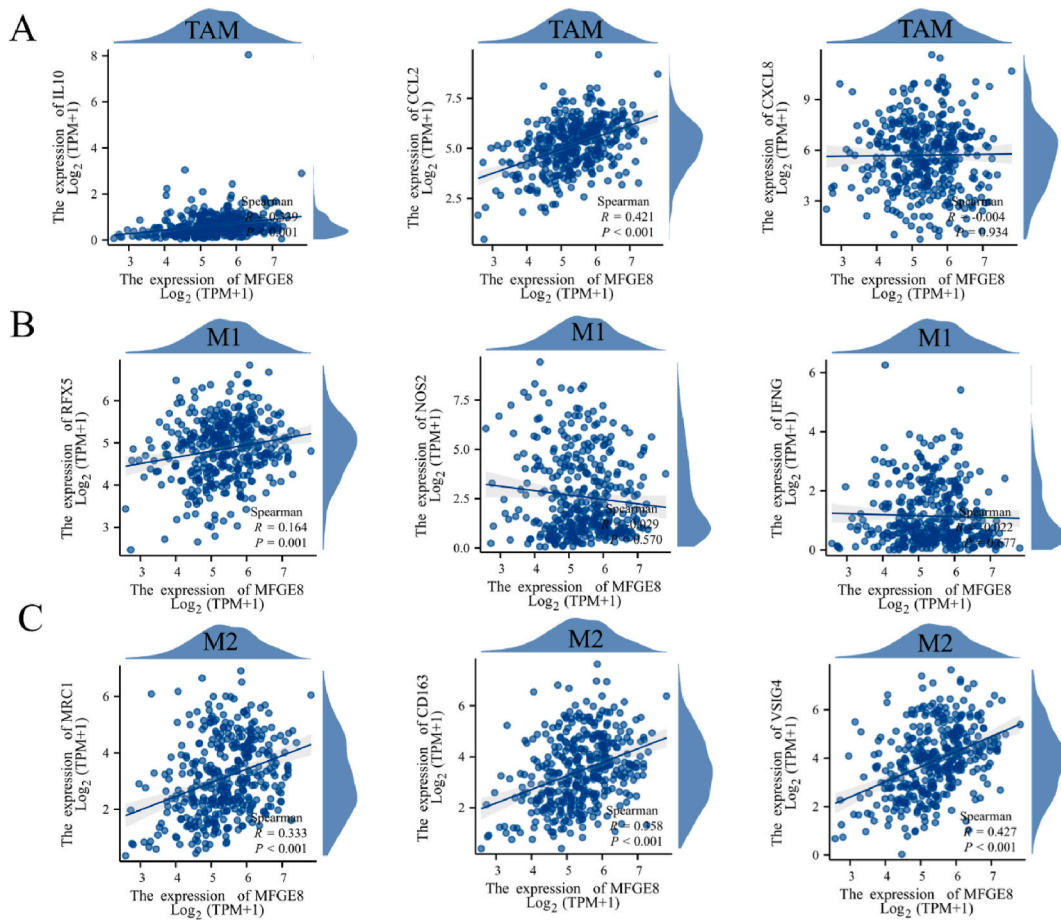
**Fig. 7.** Correlation of MFG-E8 expression with **immune infiltration cell** markers. (A) The correlation between MFG-E8 and TAM. (B) The correlation between MFG-E8 and M1 macrophages. (C) The correlation between MFG-E8 and M2 macrophages.. (CXCL8, also known as IL8; RFX5, also referred to as MHC II; NOS2, alternatively named INOS; IFNG, also recognized as IFN gamma; and MRC1, also commonly referred to as CD206.)

MFG-E8 after transfection of siRNA, and the results showed that the expression of MFG-E8 was downregulated in the AGS and MKN-45 cell lines compared with the control group (Fig. 9 A, B). The ability of cells to proliferate was then evaluated by EDU proliferation assay. The proliferative ability of AGS and MKN-45 was attenuated after MFG-E8 knockdown compared with the control (Fig. 9C, D). To assess whether MFG-E8 affects GC cell migration, we also performed a wound healing assay to further clarify. Wound healing assay showed that GC cells with knockdown of MFG-E8 exhibited weaker wound healing ability compared with the control group (Fig. 9 E, F). In addition, we carried out a Transwell invasion assay to investigate whether MFG-E8 could affect the invasion of GC cells. As we suspected, the invasiveness of AGS and MKN-45 was significantly attenuated after the knockdown of MFG-E8 compared with the control group (Fig. 9 G, H).

## 4. Discussion

In this study, we elucidated the clinical significance and expression level of MFG-E8 in GC using bioinformatics analysis. In our analysis, we have found that MFG-E8 is highly expressed in GC tissues and that high expression of MFG-E8 is correlated with poor prognosis in GC patients. Furthermore, our data show that MFG-E8 expression in GC patients also has some correlation with the immune system of the organism, especially playing a significant function in the M2 polarization of macrophages. Therefore, our study offers new insights into the critical function of MFG-E8 in GC, which may be a prognostic marker associated with immune levels in GC patients.

We evaluated the expression of MFG-E8 in GC using TCGA and GEO databases. Our analysis showed that MFG-E8 was highly expressed in GC compared with normal para-cancerous tissues. In addition, we performed a WB analysis of the GC cells and the results were consistent with the database analysis. We collected clinical samples from GC patients for IHC experiments and found that MFG-E8 expression levels were higher in most samples than in paired paraneoplastic samples. These findings suggest that MFG-E8 may be a diagnostic marker for GC. Furthermore, to further analyze whether MFG-E8 may be a prognostic marker for GC, we analyzed the association between MFG-E8 expression and overall patient survival using KM. The results showed that the expression of MFG-E8 is
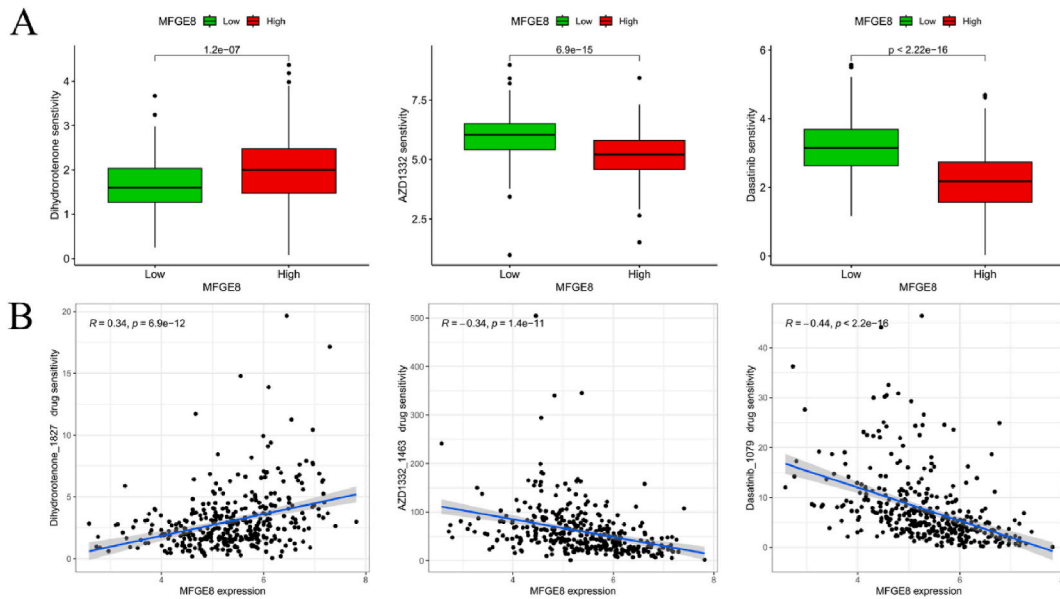
**Fig. 8.** Relationship between MFG-E8 expression in GC and chemotherapeutic drugs. (A) Low and high expression MFG-E8 pairs Box plots of IC50 for Dihydrorotenone, AZD1332, Dasatinib. (B) The relationship between MFG-E8 expression and drug sensitivity.

negatively correlated with the prognosis of GC patients, and the up-regulation of MFG-E8 is related to the poor state of GC. Taken together, these findings strongly support our hypothesis that MFG-E8 is a novel biomarker for GC. Consistent with our previous data the knockdown of MFG-E8 significantly reduces cell proliferation, migration, and invasion in GC cell lines. In follow-up studies, we will conduct further in vivo experiments to elucidate the possible mechanism of MFG-E8 involvement in GC phenotypic changes.

Furthermore, through a series of data analyses, the present study found that MFG-E8 expression was closely related to the immune status of GC patients, especially macrophage M2 polarization. In the tumor microenvironment, the enrichment and activation of immune infiltrating cells are closely related to tumor progression, and tumor immune status is a key factor determining the prognosis of patients. It has been found that MFG-E8 is secreted by activated macrophages, which bind to apoptotic cells and carry them into phagocytes for phagocytosis. In addition, MFG-E8 is clearly associated with macrophages in many aspects, such as inflammation, tumor, and immune tolerance [19,23]. It is not clear whether the expression of MFG-E8 is related to the immune infiltration of GC. When we analyzed by CIBERSORT, ssGSEA algorithm, we found that MFG-E8 expression was significantly correlated with macrophages and NK cells. However, many researchers have explored the relationship between MFG-E8 and macrophages, but the role of MFG-E8 in NK cells has not been studied.

Macrophages are Hapten cells that exist widely in the body and can be divided into M1 and M2 macrophages. Macrophages can stimulate angiogenesis, enhance the migration and invasion of tumor cells, inhibit anti-tumor immunity, and thus promote the development of cancer and malignant progression [24]. This may be due to genetic changes in the tumor microenvironment that are initiated by cancer cells or immune helper cells during tumor progression, with macrophages exhibiting predominantly M2-type polarization; It exhibits an immunosuppressive tumor phenotype and promotes tumor progression, metastasis, and treatment resistance. MFG-E8 expression has been found to be associated with M2 polarization in a variety of cancers, including the oral cavity, prostate, and melanoma [25]. In our study, we found that MFG-E8 can promote the transformation of macrophages from GC patients to M2. Further analysis of the TIMER database showed that the expression of macrophages was negatively correlated with the prognosis of GC patients. This also suggests from another perspective that MFG-E8 influences tumor progression and ultimately prognosis by promoting macrophage M2 polarization.

In addition, we performed gene enrichment to speculate on the potential mechanism of MFG-E8. KEGG analysis showed that MFG-E8 was associated with Neuroactive ligand-receptor interaction, cAMP signaling pathway, and Cholinergic synapse [26,27]. The cAMP signaling pathway is a classical oncogenic pathway [28]. It has been found that the cAMP signaling pathway can promote M2 polarization of macrophages and promote tumor progression [29]. We also analyzed the sensitivity of MFG-E8 in GC cells to chemotherapy drugs, screening out its sensitivity to Dasatinib and AZD1332. Research on AZD1332 is relatively limited, whereas Dasatinib is a commonly used antitumor drug. Dasatinib is a classical Src inhibitor [30]. Src, a tyrosine kinase receptor, is involved in several cancer-related signaling pathways [31]. For instance, Src plays a crucial role in cAMP signaling, and we speculate that the high expression of MFG-E8 may lead to an increase in cAMP phosphorylation, subsequently increasing the levels of Src. Furthermore, Dasatinib is an inhibitor of Src. In conclusion, we hypothesize that the high expression of MFG-E8 may enhance the sensitivity of GC patients to Dasatinib, possibly through the upregulation of Src levels [32]. Taken together, we hypothesized that Dasatinib use in GC patients with high expression of MFG-E8 would delay tumor progression by inhibiting M2 macrophage polarization.

However, our current research still has some deficiencies. Most of the data is based on database predictions and is constantly
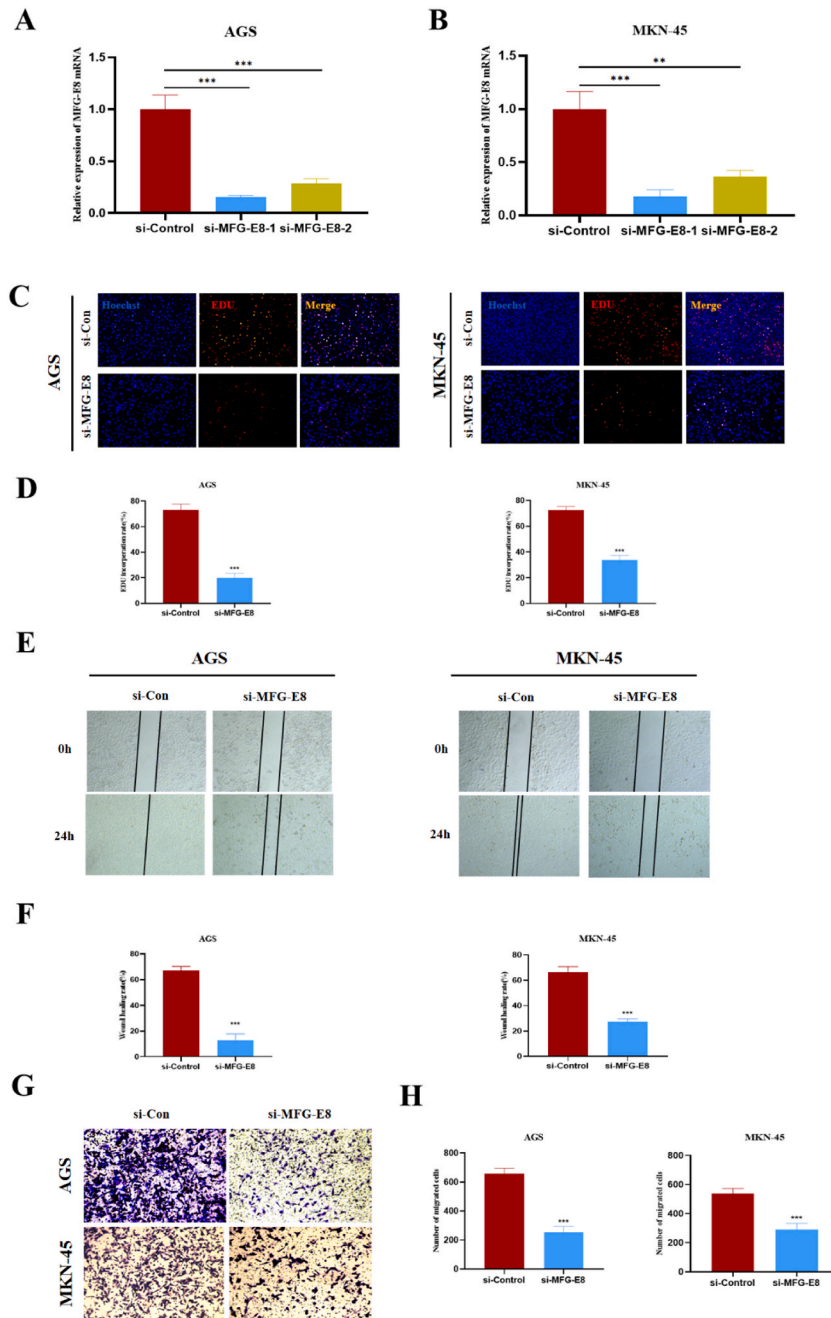
**Fig. 9.** Knockdown of MFG-E8 inhibited cell proliferation, migration, and invasion. (A, B) Expression levels of MFG-E8 in AGS and MKN45 after siRNA transfection. (C, D) EDU proliferation assay was used to detect the effect of siRNA transfection on cell proliferation. (E, F) After siRNA transfection, scratches were performed, and the healing area was recorded at 0 and 24 h, showing the effect on migration ability. (G, H) After the knockdown of MFG-E8, the effect of MFG-E8 on cell migration and invasion was examined by Transwell assay. $**p < 0.01$, $***p < 0.001$.

updated and expanded, so research results may be affected. Nevertheless, in future studies, we will explore the detailed mechanisms in more detail and conduct experiments to further validate the predicted results.

## 5. Conclusion

Overall, we found increased expression of MFG-E8 in samples from GC patients and correlated with the clinical stage of the patients. The high expression of MFG-E8 is closely related to the poor prognosis of GC. Notably, MFG-E8 expression was positively correlated with macrophage infiltration. In particular, the expression of MFG-E8 was significantly correlated with M2 polarization. In

addition, based on OncoPredict, we observed that GC patients with high MFG-E8 expression showed sensitivity to Dasatinib. Therefore, MFG-E8 may become a new marker of GC, but the potential mechanism to promote the development of GC remains to be further studied.

## Funding

## Data availability statement

The results shown in this manuscript are based upon the data generated by the TCGA Research Network: (https://www.cancer.gov/ccg/research/genome-sequencing/tcga), NCBI GEO database (GSE54129, GSE79973):(https://www.ncbi.nlm.nih.gov/geo/geo2r/?acc=), The Human Protein Atlas (https://www.proteinatlas.org/), TIMER database (https://cistrome.shinyapps.io/timer/), GDSc database (https://osf.io/c6tfx/).

## Ethics approval and consent to participate

All the experiments were approved by the Ethics Committee of the First Affiliated Hospital of Anhui Medical University. The study was the Declaration of Helsinki. Project Approval Number: PJ-YX2022-038.

## CRediT authorship contribution statement

**Yang Li:** Writing - review & editing, Writing - original draft, Visualization, Validation, Supervision, Software, Resources, Project administration, Methodology, Investigation, Funding acquisition, Formal analysis, Data curation, Conceptualization. **Jianda Qiu:** Resources, Funding acquisition, Data curation. **Ziyu Meng:** Methodology. **Shiyuan Yin:** Methodology, Investigation. **Mingxuan Ruan:** Project administration, Methodology, Investigation. **Wenbiao Zhang:** Project administration, Methodology, Investigation. **Zhiwei Wu:** Resources, Project administration, Methodology, Conceptualization. **Tao Ding:** Software, Resources, Project administration. **Fei Huang:** Writing - review & editing, Writing - original draft, Software, Resources, Project administration, Investigation, Formal analysis, Data curation, Conceptualization. **Wenbin Wang:** Writing - review & editing, Writing - original draft, Visualization, Validation, Supervision, Software, Resources, Project administration, Methodology, Investigation, Funding acquisition, Formal analysis, Data curation, Conceptualization.

## Declaration of competing interest

The authors declare that they have no known competing financial interests or personal relationships that could have appeared to influence the work reported in this paper.

## Acknowledgments

## Appendix A. Supplementary data

Supplementary data to this article can be found online at https://doi.org/10.1016/j.heliyon.2023.e23917.

## References

[1] E. Haque, et al., Recent trends and advancements in the diagnosis and management of gastric cancer, Cancers 14 (22) (2022).
[2] W.L. Guan, Y. He, R.H. Xu, Gastric cancer treatment: recent progress and future perspectives, J. Hematol. Oncol. 16 (1) (2023) 57.
[3] W. Xu, Z. Yang, N. Lu, Molecular targeted therapy for the treatment of gastric cancer, J. Exp. Clin. Cancer Res. 35 (2016) 1.
[4] X.J. Shi, Y. Wei, B. Ji, Systems biology of gastric cancer: perspectives on the omics-based diagnosis and treatment, Front. Mol. Biosci. 7 (2020) 203.
[5] L. Zhang, et al., Milk fat globule-epidermal growth factor-factor 8 improves hepatic steatosis and inflammation, Hepatology 73 (2) (2021) 586–605.
[6] W.L. Yang, et al., Milk fat globule epidermal growth factor-factor 8-derived peptide attenuates organ injury and improves survival in sepsis, Crit. Care 19 (2015) 375.
[7] A.D. Fuller, L.J. Van Eldik, MFG-E8 regulates microglial phagocytosis of apoptotic neurons, J. Neuroimmune Pharmacol. 3 (4) (2008) 246–256.
[8] A. Pritchard, et al., Lung tumor cell-derived exosomes promote M2 macrophage polarization, Cells 9 (5) (2020).
[9] M. Aziz, et al., Review: milk fat globule-EGF factor 8 expression, function and plausible signal transduction in resolving inflammation, Apoptosis 16 (11) (2011) 1077–1086.

[10] E. Albus, et al., Milk fat globule-epidermal growth factor 8 (MFG-E8) is a novel anti-inflammatory factor in rheumatoid arthritis in mice and humans, J. Bone Miner. Res. 31 (3) (2016) 596–605.

[11] M. Jinushi, et al., MFG-E8-mediated uptake of apoptotic cells by APCs links the pro- and antiinflammatory activities of GM-CSF, J. Clin. Invest. 117 (7) (2007) 1902–1913.

[12] Y. Lu, et al., MFG-E8 regulated by miR-99b-5p protects against osteoarthritis by targeting chondrocyte senescence and macrophage reprogramming via the NF-kappaB pathway, Cell Death Dis. 12 (6) (2021) 533.

[13] C. Carrascosa, et al., MFG-E8/lactadherin regulates cyclins D1/D3 expression and enhances the tumorigenic potential of mammary epithelial cells, Oncogene 31 (12) (2012) 1521–1532.

[14] M. Jia, et al., Prognostic correlation between MFG-E8 expression level and colorectal cancer, Arch. Med. Res. 48 (3) (2017) 270–275.

[15] N. Li, et al., The expression levels and clinical significance of MFG-E8 and CD133 in epithelial ovarian cancer, Gynecol. Endocrinol. 36 (9) (2020) 803–807.

[16] J.Y. Zhao, et al., Down-regulation of MFG-E8 by RNA interference combined with doxorubicin triggers melanoma destruction, Clin. Exp. Med. 15 (2) (2015) 127–135.

[17] Y. Yang, J. Guo, L. Huang, Tackling TAMs for cancer immunotherapy: it's nano time, Trends Pharmacol. Sci. 41 (10) (2020) 701–714.

[18] Y. Yuan, et al., The double-edged sword effect of macrophage targeting delivery system in different macrophage subsets related diseases, J. Nanobiotechnol. 18 (1) (2020) 168.

[19] Z. Zhou, et al., CCL18 secreted from M2 macrophages promotes migration and invasion via the PI3K/Akt pathway in gallbladder cancer, Cell. Oncol. 42 (1) (2019) 81–92.

[20] J. Ren, et al., Schwann cell-derived exosomes containing MFG-E8 modify macrophage/microglial polarization for attenuating inflammation via the SOCS3/STAT3 pathway after spinal cord injury, Cell Death Dis. 14 (1) (2023) 70.

[21] K. Yamada, et al., MFG-E8 drives melanoma growth by stimulating mesenchymal stromal cell-induced angiogenesis and M2 polarization of tumor-associated macrophages, Cancer Res. 76 (14) (2016) 4283–4292.

[22] L. Yu, et al., MFG-E8 overexpression is associated with poor prognosis in breast cancer patients, Pathol. Res. Pract. 215 (3) (2019) 490–498.

[23] W. Huang, et al., MFG-E8 accelerates wound healing in diabetes by regulating "NLRP3 inflammasome-neutrophil extracellular traps" axis, Cell Death Dis. 6 (2020) 84.

[24] L. Liu, et al., Leveraging macrophages for cancer theranostics, Adv. Drug Deliv. Rev. 183 (2022), 114136.

[25] K. Geoffroy, et al., High levels of MFG-E8 confer a good prognosis in prostate and renal cancer patients, Cancers 14 (11) (2022).

[26] H. Zhang, et al., Blockade of AMPK-mediated cAMP-PKA-CREB/ATF1 signaling synergizes with aspirin to inhibit hepatocellular carcinoma, Cancers 13 (7) (2021).

[27] J. Liu, et al., Network pharmacology-based analysis of the effects of corydalis decumbens (thunb.) pers. In non-small cell lung cancer, Evid Based Complement Alternat Med 2021 (2021), 4341517.

[28] J.Z. Zhang, et al., Phase separation of a PKA regulatory subunit controls cAMP compartmentation and oncogenic signaling, Cell 182 (6) (2020), 1531-1544 e15.

[29] D. Klaver, et al., The P2Y(11) receptor of human M2 macrophages activates canonical and IL-1 receptor signaling to translate the extracellular danger signal ATP into anti-inflammatory and pro-angiogenic responses, Cell. Mol. Life Sci. 79 (10) (2022) 519.

[30] D. Leveque, et al., Clinical pharmacokinetics and pharmacodynamics of Dasatinib, Clin. Pharmacokinet. 59 (7) (2020) 849–856.

[31] A.R. Nam, et al., Src as a therapeutic target in biliary tract cancer, Mol. Cancer Therapeut. 15 (7) (2016) 1515–1524.

[32] J. Chen, et al., Bufalin targets the SRC-3/MIF pathway in chemoresistant cells to regulate M2 macrophage polarization in colorectal cancer, Cancer Lett. 513 (2021) 63–74.